energies

MDPI

Article

Formation of Graphite-Copper/N-Silicon Schottky Photovoltaic Diodes Using Different Plasma Technologies

Žydrūnas Kavaliauskas [1,2,*], Vilius Dovydaitis [3], Romualdas Kėželis [1], Liutauras Marcinauskas [1,3], Vitas Valinčius [1], Arūnas Baltušnikas [4], Aleksandras Iljinas [3], Giedrius Gecevičius [2] and Vytautas Čapas [2]

[1] Plasma Processing Laboratory, Lithuanian Energy Institute, Breslaujos Str. 3, LT-44403 Kaunas, Lithuania; romualdas.kezelis@lei.lt (R.K.); liutauras.marcinauskas@lei.lt (L.M.); Vitas.Valincius@lei.lt (V.V.)
[2] Department of Industrial Engineering and Robotics, Kaunas University of Applied Sciences, Pramones Ave. 20, LT-50468 Kaunas, Lithuania; giedrius.gecevicius@go.kauko.lt (G.G.); vytautas.capas@go.kauko.lt (V.Č.)
[3] Department of Physics, Kaunas University of Technology, Studentų Str. 50, LT-44249 Kaunas, Lithuania; vilius.dovydaitis@ktu.lt (V.D.); aleksandras.iljinas@ktu.lt (A.I.)
[4] Laboratory of Materials Research and Testing, Lithuanian Energy Institute, Breslaujos Str. 3, LT-44403 Kaunas, Lithuania; arunas.baltusnikas@lei.lt
* Correspondence: zydrunas.kavaliauskaslei@gmail.com; Tel.: +370-37-401895; Fax: +370-37-351271

Abstract: Plasma spraying and magnetron sputtering were used to form graphite–copper films on an n-type silicon surface. The main objective of this work was to compare the properties of the obtained graphite–copper Schottky photodiodes prepared using two different layer formation methods and to evaluate the influence of copper content on the surface morphology, phase structure, and photovoltaic characteristics of the graphite–copper films. Surface morphology analysis shows that the surface of the formed layers using either plasma spraying technology or the magnetron sputtering method consists of various sphere-shaped microstructures. The X-ray diffraction measurements demonstrated that the graphite–copper coatings formed by plasma spraying were crystalline phase. Meanwhile, the films deposited by magnetron sputtering were amorphous when the copper concentration was up to 9.7 at.%. The increase in copper content in the films led to the formation of Cu crystalline phase. Schottky diodes formed using magnetron sputtering technology had a maximum current density of 220 mA/cm^2 at 5 V. Meanwhile, the maximum electric current density of Schottky photodiodes formed using plasma spraying reached 3.8 mA/cm^2. It was demonstrated that the efficiency of Schottky diodes formed using magnetron sputtering was up to 60 times higher than Schottky diodes formed using plasma spraying.

Keywords: plasma spraying; magnetron sputtering; copper; graphite; Schottky photodiodes; photovoltaic

Citation: Kavaliauskas, Ž.; Dovydaitis, V.; Kėželis, R.; Marcinauskas, L.; Valinčius, V.; Baltušnikas, A.; Iljinas, A.; Gecevičius, G.; Čapas, V. Formation of Graphite-Copper/N-Silicon Schottky Photovoltaic Diodes Using Different Plasma Technologies. *Energies* **2021**, *14*, 6896. https://doi.org/10.3390/en14216896

Academic Editor: Gregorio García

Received: 31 August 2021
Accepted: 8 October 2021
Published: 21 October 2021

1. Introduction

In recent years, a number of studies related to the semiconductor (P-N) junction or the metal semiconductor junction (Schottky diodes) have been carried out, as well as experimental and theoretical studies of solar cells formed using these structures [1–5]. The technological reliability of these structures depends in particular on the peculiarities of the formation, for example: the properties of the metal–semiconductor interface at the junction, the heterogeneity of Schottky barrier contacts, and the resistance of serial diodes to environmental influences. In order to form high-quality Schottky diode heterojunctions suitable for the production of photovoltaic cells, it is necessary to use metals with low surface energy (up to 3–4 eV) that allow for the easy release of electric charge carriers while interacting with sunlight [5–7].

Compared to typical p-n junction diodes, Schottky diodes can pass higher currents and, depending on the height of the barrier, have a saturation current that is several orders

of magnitude higher. For these reasons, Schottky diodes are more commonly used in areas where high currents and low voltages are required. A major advantage of the Schottky diodes is that they do not have side charge carriers, which eliminates the problem of their recombination, which is relevant to p-n diodes. This means that Schottky diodes are faster and more suitable to use in digital logic circuits. Rapid Schottky photodiodes are used for optical communications and optical measurements as well as in cheap solar cells [8–12].

Because the solar cells are usually exposed to a variety of outdoor conditions, they must be resistant to environmental influences or contain an additional protective layer that lowers the interaction of light with Schottky junctions. Such design features of photovoltaic cells increase the cost of solar cells and reduce the efficiency. To avoid these shortcomings, attempts have been made to look for solutions using different composites of materials [8–14]. One such composite is a graphite–copper layer [15–21]. The copper in the composite ensures good electrical conductivity and sufficient plasticity, while the graphite provides good resistance to environmental influences (e.g., air humidity, temperature fluctuations). In addition, these materials are quite cheap compared with others used in the production of photovoltaic cells. The copper in the composite ensures good contact with the silicon surface. In this way, it is possible to form high-quality Schottky photodiodes suitable for the production of solar cells. A solar cell with the required power can be obtained using Schottky diode arrays and a mixed electrical connection. Various technologies are used to form graphite–copper composites or composite coatings, such as hot pressing sintering, electroless plating, magnetron sputtering, and plasma spraying [15–25].

Using plasma spraying technology, the formation of the coating or composite coating on the substrate is fairly rapid (about 1–3 min), while the injection of the primary powder mixture into the plasma generator chamber is performed using special dispensers of the powder mixture mixed at the required ratio. Sufficient adhesion between the coating and the substrate (e.g., a Si substrate) is ensured by selecting appropriate technological parameters, such as plasma flow temperature, plasma-forming gas flow rate, and coating formation time [24,26–28].

Magnetron sputtering enables us to control the thickness of the deposited layer with sufficient precision, which saves materials used in the production of photovoltaic cells. The main disadvantage of this technology is that the process of forming the composite layer takes up to several hours as a deep vacuum must be achieved in the vacuum chamber beforehand [20–23].

This work was performed because there is a lack of data in the scientific literature on the employment of plasma spraying for the production of Schottky photodiodes. Thus, there are no data on the comparison of plasma spraying's suitability and magnetron sputtering's suitability for the formation of Schottky photodiodes. The graphite–copper mixture was chosen in order to avoid the copper's oxidation as much as possible and to prolong the lifecycle of the batteries and their resistance to the environment. The main factor determining the performance of Schottky photodiodes is the copper-to-graphite ratio in the composite.

The aim of this research is to find the optimal elemental composition of graphite–copper composite films at which the Schottky photodiodes prepared using plasma spraying and magnetron sputtering technologies would have the highest properties.

2. The Experimental Setup

Plasma spraying technology was used to form the coatings for Schottky photodiodes. The plasma spraying technological stand was developed and tested in the Plasma Processing Laboratory of the Lithuanian Energy Institute (Kaunas, Lithuania) [24]. Schottky photodiodes were deposited using graphite and copper feedstock powder mixtures. The copper powders used for the spraying were ~44 μm in size and of 99% purity (Alfa Aesar GmbH, Karlsruhe, Germany). The graphite powders used for the deposition were of an irregular shape (mark JX-NGF2, J&X Tech Co., Ltd. Shenzhen, China). The graphite powder size range was determined by sieving the initial powder using 150 μm and 20 μm

meshes and separating larger and smaller particles from the powder. The specific surface area of the graphite powder was about 1.84 m^2/g. The amounts of copper in the feedstock powder mixtures were 10 wt.% (Gr-10Cu), 20 wt.% (Gr-20Cu), 40 wt.% (Gr-40Cu), and 60 wt.% (Gr-60Cu). Graphite (Gr) or copper (Cu) coatings using only the copper or graphite powder were also formed. The graphite and copper powders were mixed using a powder mixer. The mixing process lasted for 12 h. The coatings were formed on n-type silicon substrates with a thickness of 500 µm, a specific resistance of 100 $\Omega \times cm^{-1}$, and crystallographic orientation <100>. The feedstock powder was injected tangentially into the plasma generator using a special dosing system. The layers were formed at a plasma generator arc current of 200 A and a power of ~17.0 kW using argon gas. The distance between the plasma generator nozzle's exit and the surface of the cooled Si substrate was 75 mm. The deposition duration was 60 s.

Carbon–copper thin films were grown on a silicon substrate using a layer-by-layer direct current (DC) magnetron deposition method [29]. The films were grown using two flat magnetrons, each equipped with 3-inch diameter graphite and copper targets (from Kurt. J. Lesker Company). They were aligned to be at the same height, parallel to each other. Deposition was done in a 1 Pa argon environment at a substrate temperature of 400 °C. The substrate holder moved parallel to the targets in a pendulum-like motion at a frequency of 0.3 Hz. When the substrate moved above each operating magnetron, a layer of atoms was deposited on the Si substrate. The substrate was positioned to be at a distance of 65 mm from the targets. Several series of thin films were deposited. First, a film (MS1) using only the graphite target at a 1.5 A current was sputtered. The carbon–copper composite films MS2 (graphite target current I = 1.5 A and Cu target current I = 0.1 A), MS3 (graphite I = 1.5 A and Cu I = 0.3 A), and MS4 (graphite I = 1.5 A and Cu I = 0.4 A) were deposited. Finally, a copper film (MS5) using only a Cu target at a fixed 0.4 A current was sputtered. The entire growth process took 20 min for all films.

A Hitachi S-3400 N scanning electron microscope (Hitachi, Tokyo, Japan) was employed to analyze the morphology of the produced coatings. The elemental composition of the coatings was estimated by energy-dispersive X-ray spectroscopy (EDS) using a Bruker Quad 5040 spectrometer (Hamburg, Germany). The coating structure was analyzed by X-ray diffraction (XRD) (DRON-UM1, with standard Bragg–Brentano focusing geometry) in a 10–100° range applying CuKα (λ = 0.154059 nm) radiation. The structure of films deposited by magnetron sputtering was measured by a D8 Discover X-ray diffractometer (Bruker ASX GmbH, Billerica, MA, USA) using the glancing (grazing) incidence configuration in a 20–55° range at a 0.2 angle of incidence.

The photovoltaic properties of the manufactured Schottky photodiodes (heterojunctions) were investigated using a Keithley 5487 multimeter. The efficiency of Schottky photodiodes was evaluated as expressed by the formula:

$$\eta = \frac{P_{out}}{P_{in}} * 100\%$$

there P_{out} is the electric power generated by the Schottky photodiodes, and P_{in} is the power of the radiation applied to the photodiode.

3. The Results of the Experiment

Figure 1 shows micro relief images of the surface of copper–graphite composite coatings when they were formed by plasma spraying. Figure 1a shows the surface of the coating formed using only the graphite powder. In this case, the surface consists of irregularly shaped microstructures and micro-islands, which were possibly formed by the sublimation of the primary powder and smashing on the surface of the silicon substrate at high speed. Figure 1b shows the surface of the coating prepared using 10 wt.% of copper in the feedstock powder. In this case, the surface is composed of irregularly shaped microstructures. As can be seen from the SEM surface image of the Gr-10Cu coating, the predominant structure is composed of irregularly shaped micro-islands. Figure 1c shows

the surface morphology of the Gr-20Cu coating. It is probable that in this case the surface of silicon is reached by a higher number of partially or fully melted copper particles, so the surface structure is composed of solid microsplats with a diameter of about 10 µm.

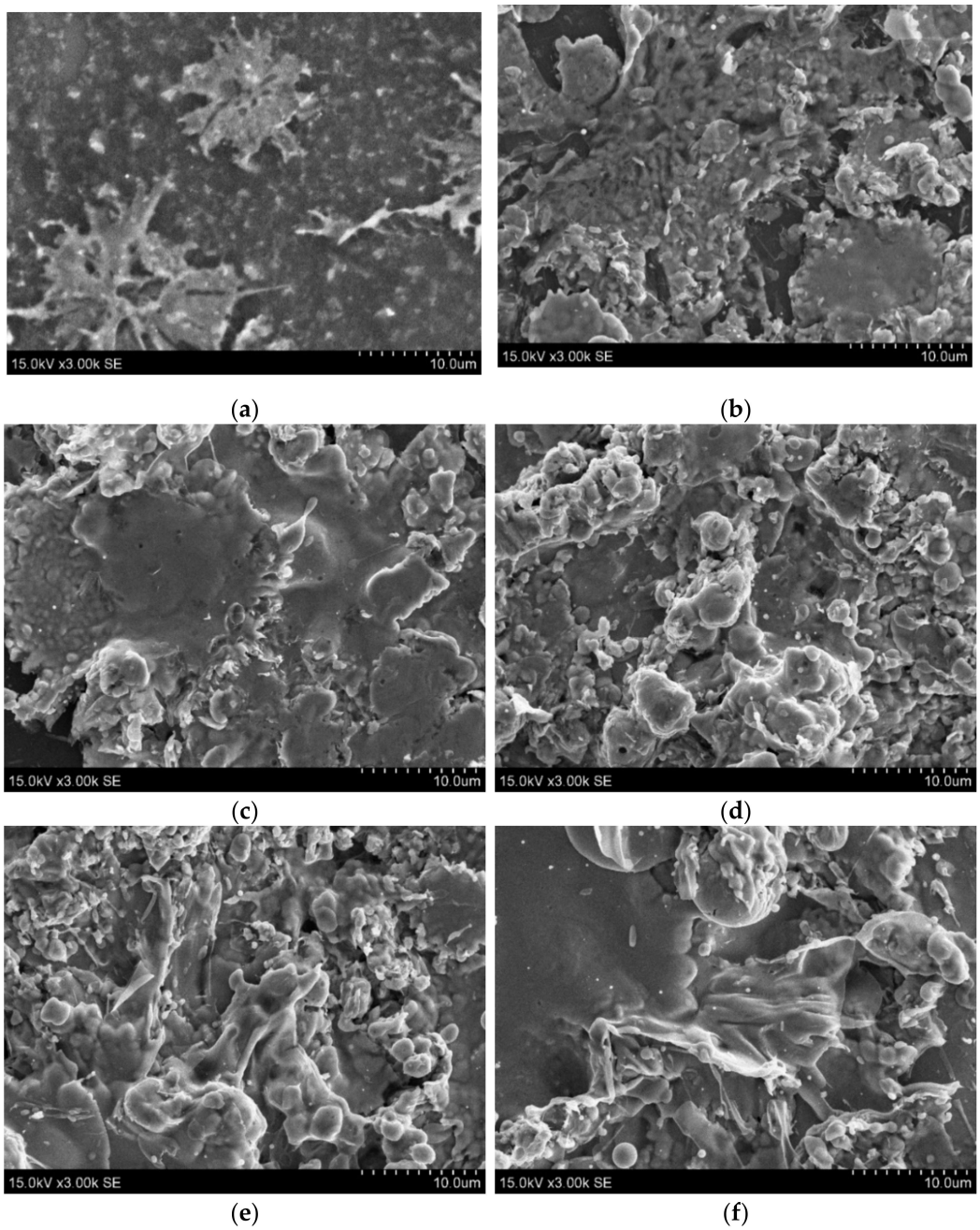

Figure 1. Surface morphology of (**a**) graphite, (**b**) Gr-10Cu, (**c**) Gr-20Cu, (**d**) Gr-40Cu, (**e**) Gr-60Cu, and (**f**) copper films deposited using plasma spraying.

Figure 1d,e show the coating surfaces when the amount of copper in the feedstock powder mixtures injected into the plasma jet during the experiment was 40 wt.% and 60 wt.%, respectively. In this case, the surface morphology is composed of various microstructures. As can be seen, some of them are spherical in shape. Such a surface structure can be explained by the fact that when copper is dominant, these particles partially or completely melt inside the plasma jet to form droplet-shaped microparticles because the droplet surface energy is the lowest. Figure 1f shows the surface of the coating sprayed using only the copper powder. In this case, the predominant structure of the surface is

composed of spherical particles with a diameter of about 1–5 μm and fully melted splats. This can be explained by the fact that, as in the Figure 1d,e cases, the surface is bombarded by completely molten copper particles that, after solidification, form sphere-shaped splats and particles of such microstructures have the lowest surface energy [24,28,30].

SEM surface images of films deposited by magnetron sputtering are presented in Figure 2. Figure 2a shows the surface morphology of the MS1 film (deposited using only a graphite cathode). As can be seen, the surface is uniform and smooth. Hence, in this case, the carbon layer is evenly distributed over the entire surface of the substrate. Figure 2b shows the surface of the MS2 film when the formation took place using two cathodes—graphite and copper. The addition of copper slightly increased the surface roughness and structures with a small size (~0.1 μm in diameter) were formed. This can be explained by the fact that, when the copper atoms reach the surface, they form droplet-shaped spherical microstructures [21,23]. Figure 2c–e shows the surfaces of the MS3 and MS4 films deposited when the copper target current was increased up to 0.3 A and 0.4 A, respectively. In both of these cases, the content of copper in the films was increased and larger-sized microstructures resembling a sphere were deposited. The diameter of the sphere-like particles forming the surfaces in this case varied in the range of 0.2–0.5 μm. It was demonstrated that the Cu clusters segregate from the carbon phase and the formation of microparticles occurs [20,21]. In addition, the incorporation and enhancement of Cu content in the carbon matrix increases the roughness of the films [20]. Figure 2f shows the surface morphology of the film when the film was formed on a silicon substrate using only a copper cathode. As can be seen, the surface is composed of irregularly shaped grains, some of which resemble irregular trapezoids. Meanwhile, the morphology of the resulting surface in this case is somewhat reminiscent of isles.

Table 1 presents the results of the EDS analysis describing the distribution of copper, carbon, silicon, and oxygen on the surface of the formed films. Table 1 presents the elemental composition when the films were formed using magnetron sputtering and plasma spraying techniques without and with elimination of the Si substrate's influence. Analysis of the EDS results shows that the oxygen content is 2.3 at.% in the MS1 film. Such an amount of oxygen is influenced by the fact that the deposition was performed at a pressure of ~1 Pa and in the small amount of residual air that was left in the vacuum chamber. The highest concentration of oxygen (~18.2 at.%) was obtained when the copper film was deposited. When using magnetron sputtering for the formation of copper coatings, some of the copper can be converted into copper oxide or copper silicide at higher temperatures [31,32]. The highest oxygen content of 6.5 at.% was obtained in the graphite film when the deposition of coatings was done by plasma spraying technology. This can be explained by the fact that, during the formation of graphite coatings, the surface develops a porous structure and oxygen is absorbed onto the surface of the formed micropores. Meanwhile, the introduction of additional copper particles into the plasma jet (when the copper content in the feedstock powder ranged from 10 to 60 wt.%) reduced the amount of oxygen by about 2 times and reached about ~3.0 at.% for all samples.

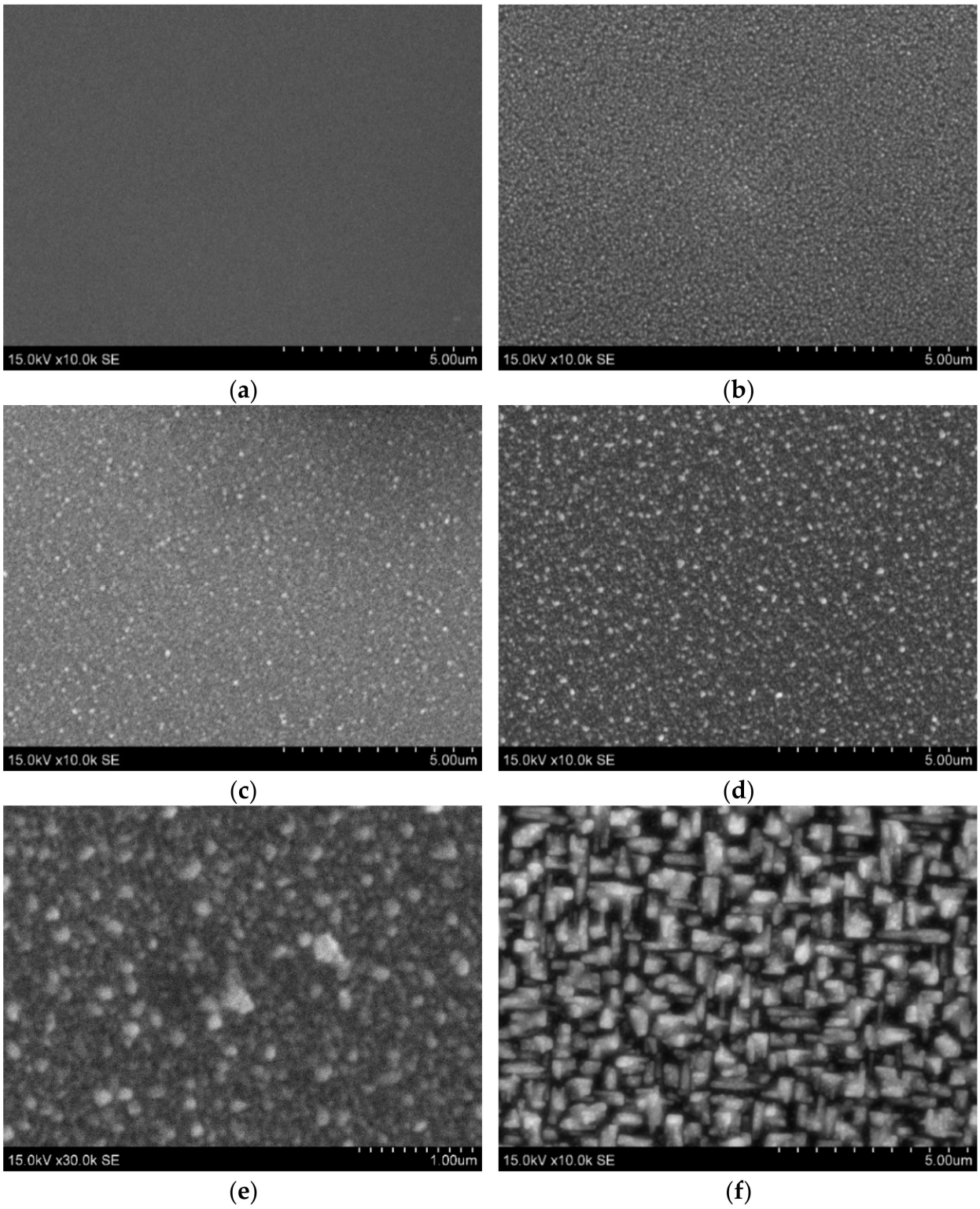

Figure 2. Surface morphology of the (**a**) MS1, (**b**) MS2, (**c**) MS3, (**d**,**e**) MS4, and (**f**) MS5 films obtained using magnetron sputtering.

Table 1. Elemental composition of films formed using magnetron sputtering and plasma spraying (as deposited and recalculated with the elimination of Si).

Coating	C, at.%	Cu, at.%	O, at.%	Si, at.%	C, at.%	Cu, at.%	O, at.%
MS1	22.3	0	2.3	75.4	90.7	0	9.3
MS2	23.3	2.8	2.9	71.0	80.3	9.7	10.0
MS3	8.6	2.6	1.5	87.3	67.8	20.6	11.6
MS4	16.2	17.3	7.2	59.3	39.8	42.4	17.8
MS5	2.6	19.6	18.2	59.6	6.5	48.5	45.0
Gr	49.6	2.9	6.5	40	84.0	5.0	11.0
Gr-10Cu	4.2	30.2	2.9	62.6	11.2	81.0	7.9
Gr-20Cu	3.5	29.4	3.1	63.8	9.7	81.6	8.6
Gr-40Cu	29.0	47.6	2.9	20.5	36.5	59.9	3.6
Gr-60Cu	20.7	44.7	2.8	31.8	30.4	65.5	4.1
Cu	0	88.5	2.6	8.9	0	97.1	2.9

However, in order to determine the actual composition of deposited films, the Si content was removed (Table 1). It was found that the MS1 film consisted of carbon (~90.7 at.%) and oxygen (9.3 at.%). Meanwhile, the oxygen concentration remained similar (~10.0 at.%) when a low amount of copper (~9.7 at.%) was inserted into the MS2 film. It should be noted that the concentration of the oxygen was slightly enhanced to 11.6 at.% when the copper content reached 20.6 at.% in the film (Table 1). However, the oxygen content was ~17.8 at.% when the concentrations of copper and carbon in the film were almost equal (~42.4 at.% and 39.8 at.%, respectively). Meanwhile, when planning to obtain a coating (MS5) with 100 at.% of copper, the results of the EDS measurements show that, after the experiment, the copper content reached about 48.5 at.% and the oxygen concentration was ~45.0%. Such a large amount of oxygen in the film indicates that some of the copper had been converted to copper oxide.

When the coatings were fabricated using plasma spraying technology, the EDS studies show that about 5.0 at.% of the copper content was obtained since a small portion of the copper entered from the plasma generator's parts even though the primary powder consisted only of graphite. When increasing the copper concentration in the feedstock powder from 10 to 60 wt.%, the analysis of the EDS results shows a significant discrepancy in the copper content in the films. In this case, the copper content in the Cr-10Cu, Gr-20Cu, Gr-40Cu, and Gr-60Cu films ranges from 59.9 to 81.6 at.% (Table 1). This result is mainly influenced by the fact that the elemental composition of the formed layer does not coincide with the composition of the feedstock graphite–copper powder. The copper particles are heavier than graphite and the melting temperature of copper is only 1360 K. Meanwhile, the sublimation of graphite starts at 3000 K, but the melting point is ~3870 K, at which point graphite sublimates rather than melts [30,33]. Thus, the injected copper particles would be fully or partially melted in the plasma jet as they reach the surface of the substrate. As a result, the impacting copper particles stick to the substrate and solidify [24,28,30]. Meanwhile, the graphite particles remain in the solid phase and only the size of particles reduces due to the partial sublimation.

The lowest amount of oxygen (~2.9 at.%) was obtained in the coating when the pure copper powder was used (Table 1). Such a result indicates that only a small amount of copper was converted to copper oxide or that oxygen was absorbed only on the surface of the coating because inert argon gas was used to create the plasma [24]. D.K. Christoulis et al. [30] found that the oxygen content in plasma-sprayed copper coatings depends on the temperature of the substrate. The oxygen concentration increased from ~3.5% to ~10% with the increase in the substrate's temperature from 200 °C to 300 °C. A. Ranjan et al. [28] obtained the formation of a low amount of cuprous oxide due to the oxidation of copper powder in plasma-sprayed copper coatings. It should be noted that the plasma spraying parameters were kept constant during all experiments. Thus, the substrate temperature

should have remained constant and did not have a significant effect on the oxidation rate of copper.

The XRD studies and analysis revealed that the formed carbon, carbon–copper, and copper layers using magnetron sputtering have amorphous structures; therefore, their roentgenograms are not presented separately. However, the crystalline phases were detected for the MS3, MS4, and MS5 films when these films were analyzed using grazing incidence X-ray diffraction (Figure 3a). The XRD pattern of the MS5 film demonstrated peaks at ~44.6° and 45.2°, which were attributed to the (320) and (312) planes of Cu_3Si [31,34,35]. The broader peaks at 43.4° and 50.5° are related to the (111) and (200) planes of face-centered cubic copper [20,31,32,34,35]. The low intensity peaks at ~49.7° and 51.3° could be attributed to Cu_3Si phase [36]. Meanwhile, the MS3 and MS4 films demonstrated two broad diffraction peaks at 43.4° and 50.5° corresponding to the (111) and (200) planes of copper (Figure 3a) [31,32]. It should be noted that the low intensity and broad peak at ~45.4° attributed to $Cu_{0.83}Si_{0.17}$ was also obtained [34]. Meanwhile, the MS2 film (Cu-9.7 at.%) was amorphous. It was obtained, that the transformation from the uniform smooth amorphous-like film structure to the fine grain features, followed by the growth of the grains for Cu films with increasing film thickness from 130 nm to 1050 nm [25]. Meanwhile, the Cu films were mostly amorphous in nature when the thickness was 500 nm or the carbon-copper films consisted of a low amount of copper [20,25].

Figure 3b presents XRD studies where graphite–copper coatings were formed using plasma spraying technology. It should be noted that the Si (400) substrate Brag peaks that were obtained at ~21.8°, 33.1°, and 69.2° are related to the λ/3, λ/2, and λ harmonic radiations, respectively. During the formation of the layers, the copper content in the feedstock powder varied from 0 to 100 wt.%. The XRD patterns show copper-specific peaks at 43.4°, 50.5°, 74.3°, 90.1°, and 95.4° attributed to the (111), (200), (220), (311), and (222) crystalline planes of copper, respectively (Figure 3b) [24,27,28]. The copper crystallite structure was cubic (Fm3m space group, no. 225 (pdf. no. 4-836)). At the value of ~26.6 degrees, a peak characteristic of crystalline graphite (002) was observed (pdf. no. 75-2078) [24]. Analyzing the XRD results, it can be stated that the variation in the copper content in the layers of the Schottky diodes did not affect the crystalline structure of the material. Analysis of XRD spectra revealed that the graphite–copper composite coatings have stresses caused by different coefficients of thermal expansion between the coating and the substrate. For this reason, it was not possible to calculate the crystalline lattice constant. An increase in the intensity of the copper peaks was observed with increase in the copper content in the coatings. The EDS studies show that a low concentration of oxygen was obtained. It led to suggestions that some of the copper was converted into copper oxide during the formation of the layers. The formation of Cu_2O in the copper coatings was observed in several studies [27,28,30]. The XRD analysis demonstrated that a large amount of cubic Cu had been retained and only a small amount of Cu_2O had been formed. In addition, the fraction of copper oxide was enhanced at a higher torch power [28]. However, the peaks of copper oxide were not observed in our graphite–copper coating during the analysis of the XRD diffraction patterns (Figure 3b).

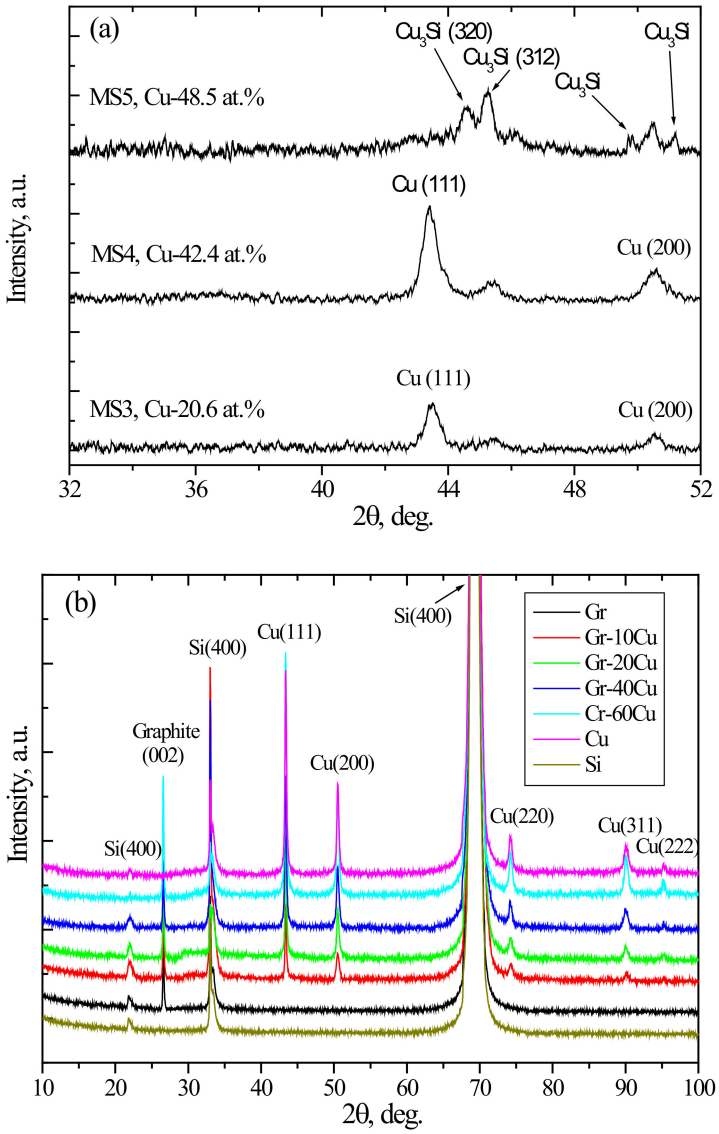

Figure 3. XRD patterns of the films deposited using (**a**) magnetron sputtering and (**b**) plasma spraying.

Figure 4 shows the photocurrent density measurements when Schottky photodiodes were formed using magnetron sputtering technology. The photocurrent density was estimated from the electric current generated by the Schottky photodiode by illuminating it with a general daylight LED-type light source. According to our studies, the lowest current density of 42 mA/cm^2 at 5 V was obtained when the Schottky diodes were deposited only from the graphite target. Meanwhile, the current density reached up to about 220 mA/cm^2 when a small amount of copper (~9.7 at.%) was introduced into the film. However, the current density value was reduced to 175 mA/cm^2 when the copper content was increased twice (MS3 film). The photocurrent density was further reduced to 70 mA/cm^2 with the increase in the copper content in the film. However, the current density was enhanced up to 220 mA/cm^2 when the copper film's deposition was done. The increase in the copper concentration from ~10 at.% to ~21 at.% and to ~42 at.% reduced the photocurrent density values. This result can be explained by the fact that increasing the copper content did not have a noticeable effect on the electrical conductivity, which is confirmed by previous studies presented in the publication [24]. At a copper content of 42 at.%, a decrease in the photocurrent density of about 3 times was observed compared with cases where the copper content is ~10 at.%. This can be explained by the formation of copper oxide and the high fraction of C=C and C=O sp^2 carbon sites. A significant amount of copper was

converted to copper oxide during the deposition or after exposure of the films to air, which has an undesirable negative effect on the current density of Schottky photodiodes. Thus, it does not ensure the good mobility of electric carriers. The mechanism that ensures the transport of carriers is photoemission, which is created by illuminating a Schottky diode with an external light source. Another phenomenon influencing the directional motion and generation of charge carriers and, thus, the shape of the photoelectric density versus voltage curve is the thermoelectric emission charge transfer mechanism, in which thermally excited electrons (or holes) enter the metal from a semiconductor by crossing a potential barrier.

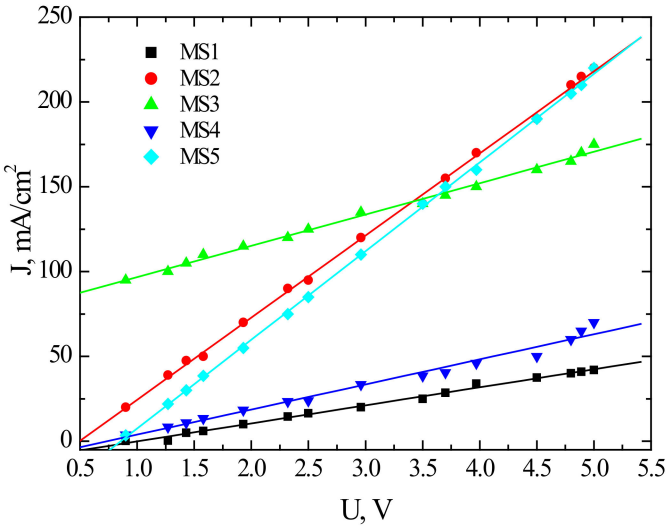

Figure 4. Photocurrent density versus voltage when films were formed by magnetron sputtering.

Figure 5 shows the photocurrent density measurements when Schottky photodiodes were formed by plasma spraying. The lowest photocurrent density of 0.69 mA/cm^2 was obtained when the Schottky photodiodes were formed using only a graphite powder. Meanwhile, after the addition of 10 wt.% of copper into the feedstock powder (the Gr-10Cu film), the photoconductive current density of the Schottky diodes reached up to 2.8 mA/cm^2. This can be explained by the fact that the added copper increased the conductivity in the Schottky heterojunction and the number of generated electrons and holes that migrated there, which decreases the barrier height. The further increase in the copper content in the feedstock powders increased the photocurrent density to 3.4 mA/cm^2. However, the current density was 3.8 mA/cm^2 and 3.4 mA/cm^2 for the Gr-40Cu and Gr-60Cu films, respectively.

It should be noted that a current density of 3.6 mA/cm^2 was obtained for the copper film. The increase in the graphite content in the Gr-40Cu and Gr-60Cu films is related to the higher copper volume fraction in the feedstock powders. In addition, copper particles have higher kinetic energy and a lower melting point than graphite ones. For this reason, copper particles are more likely to stick to the surface of the Si substrate. Thus, the Si surface is covered by melted copper splats and incoming graphite particles are trapped in them. As a result, the graphite concentration would be enhanced, but the electrical conductivity would be reduced.

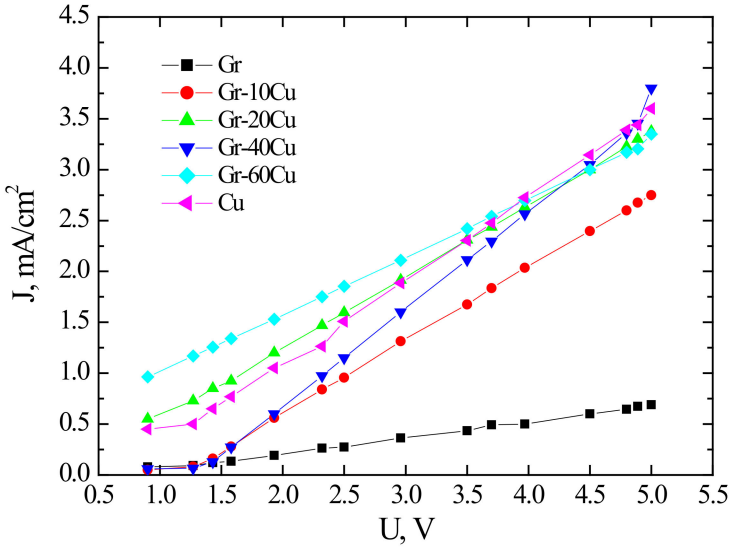

Figure 5. Photocurrent density versus voltage when films were deposited by plasma spraying.

Figure 6 shows the dependence of the Schottky photodiode's efficiency on the type of deposited film. The studies indicate that the highest efficiency of 27.5% was obtained for the MS2 and MS5 films using magnetron sputtering. Meanwhile, the lowest efficiency of 5.3% was obtained when the Schottky photodiode consisted only of amorphous carbon (the MS1 film) on a Si substrate. This change in efficiency was due to the same reasons as for the change in photocurrent density. The efficiency coefficients of Schottky diodes formed using magnetron sputtering were from 10 to 60 times higher compared with the films produced by plasma spraying. Using plasma spraying technology, the efficiency was only 0.45% when the copper powder was used. This result can be explained by the fact that the surface of the Si was not fully covered by copper and graphite particles and uncovered areas were obtained, even when only copper powder was used. Consequently, the entire surface area of the substrate was not utilized for photovoltaic generation.

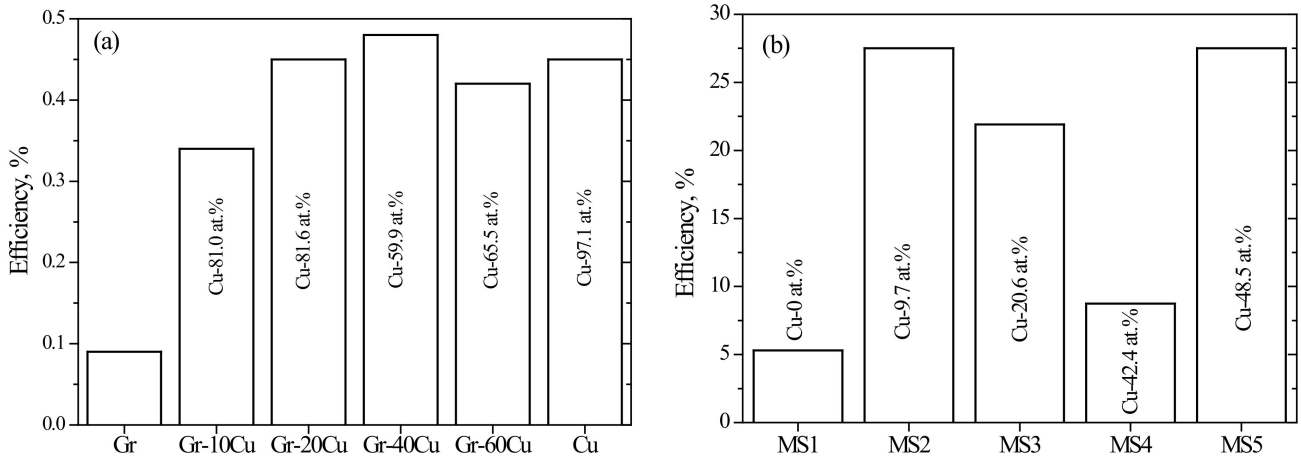

Figure 6. Variation in the Schottky photodiode efficiency of the films when deposition was performed using (**a**) plasma spraying and (**b**) magnetron sputtering.

The graphite–copper layer formed using plasma spraying technology is sufficiently thick (it can reach 50 µm and greater) to reduce the generation of the main electric carriers (electrons and holes) involved in the formation of the photocurrent. Another factor influencing the low efficiency is that when the copper particles reach the surface of the Si substrate, they partially or completely melt and, therefore, form a droplet-shaped structure

on the surface during the solidification process (as confirmed by the SEM surface studies). Therefore, such a surface structure negatively affects the number of main charge carriers involved in the photocurrent formation processes.

4. Conclusions

Schottky photodiodes were formed using two technologies, namely plasma spraying technology and magnetron sputtering technology. The surfaces of the plasma-sprayed films consisted of partly and fully melted copper splats into which were incorporated graphite particles. The quality of the graphite–copper coatings was enhanced with the increase in the copper concentration in the feedstock powders. SEM analysis shows that the surface morphology of the films deposited by magnetron sputtering is smooth and homogeneous. However, the size of the sphere-shaped microparticles increased and larger grains were formed with the increase in the copper concentration in the films. The EDS results show that the oxygen content in the graphite–copper films formed using plasma spraying technology varies in the range of 3.6–7.9 at.%. Meanwhile, the highest content of oxygen (~11 at.%) was obtained when the coating was sprayed using only the graphite powder. The EDS studies demonstrated that the oxygen content was ~9.3 at.% in the amorphous carbon film deposited by magnetron sputtering. The oxygen concentration increased from 10.0 to 17.8 at.% with the increase in the copper content in the amorphous carbon–copper composite films. The highest oxygen content (~45.0 at.%) was obtained when the Schottky diodes were formed on the Si surface using only a copper cathode. The grazing incidence angle XRD studies showed that the MS1 and MS2 films deposited using magnetron sputtering were amorphous. The MS3 and MS4 films exhibited the cubic phase of copper. The MS5 film was composed of Cu_3Si and Cu crystalline phases. The XRD results indicate that the graphite–copper and copper coatings formed by plasma spraying were of crystalline phase and the highest intensity peak at ~43.4° was attributed to the (111) plane of copper. The peak at ~26.6° was related to the (002) plane of graphite. Analysis of the light characteristics of the Schottky photodiodes showed that the highest photocurrent density values of 220 mA/cm^2 were obtained at 5 V for the MS2 and MS5 films, respectively. When Schottky photodiodes were formed using plasma spraying, their current densities ranged from 0.7 to 3.8 mA/cm^2 (at 5 V), which was much lower (up to 60 times) than that of films produced by magnetron sputtering. The highest efficiency of Schottky photodiodes of 27.5% was obtained for the MS2 and MS5 films produced by magnetron sputtering. Meanwhile, the highest efficiency of photodiodes formed using plasma spraying technology was only about 0.48% (the Gr-40Cu film). Consequently, the plasma spraying technology is not very suitable for the formation of Schottky photodiodes. However, it is superior to magnetron sputtering technology because films can be formed much faster, in just 60 s.

Author Contributions: Conceptualization, Ž.K., V.D., L.M. and A.B.; methodology, Ž.K., A.I., R.K., V.V. and V.Č.; software, A.B.; G.G. and Ž.K.; formal analysis, Ž.K., V.D., R.K., V.Č. and G.G.; investigation, V.D., A.B., A.I., L.M., R.K. and Ž.K.; data curation, Ž.K. and V.D.; writing—original draft preparation, Ž.K., V.D., A.I. and L.M. and writing—review and editing, Ž.K., V.D., L.M. and A.B.; visualization, V.D., V.Č. and G.G.; supervision, Ž.K. All authors have read and agreed to the published version of the manuscript.

Funding: This research received no external funding.

Institutional Review Board Statement: Not applicable.

Informed Consent Statement: Not applicable.

Data Availability Statement: Data sharing not applicable.

Conflicts of Interest: The authors declare no conflict of interest.

References

1. Song, L.; Yu, X.; Yang, D. A review on graphene-silicon Schottky junction interface. *J. Alloy. Compd.* **2019**, *806*, 63–70. [CrossRef]
2. Bartolomeo, A. Graphene Schottky diodes: An experimental review of the rectifying graphene/semiconductor heterojunc-tion. *Phy. Rep.* **2016**, *606*, 1–58. [CrossRef]
3. Abinay, K.; Abinaya, K.; Karthikaikuma, S.; Sudha, K.; Sundharamurthi, S.; Elangovan, A.; Kalimuthu, P. Synergistic effect of 9-(pyrrolidin-1-yl) perylene-3,4-dicarboximide functionalization of amino graphene on photocatalytic hydrogen gener-ation. *Sol. Energy Mater. Sol. Cells* **2018**, *185*, 431–438. [CrossRef]
4. Kusuma, J.; Balakrishna, R.; Patil, S.; Jyothi, M.S.; Chandan, H.R.; Shwetharani, R. Exploration of graphene oxide nanorib-bons as excellent electron conducting network for third generation solar cells. *Sol. Energy Mater. Sol. Cells* **2018**, *183*, 211–219. [CrossRef]
5. Liu, L.; Zheng, K.; Yan, Y.; Cai, Z.; Lin, S.; Hu, X. Graphene Aerogels Enhanced Phase Change Materials prepared by one-pot method with high thermal conductivity and large latent energy storage. *Sol. Energy Mater. Sol. Cells* **2018**, *185*, 487–493. [CrossRef]
6. Zhao, X.; Wu, H.; Yang, L.; Wu, Y.; Sun, Y.; Shang, Y.; Cao, A. High efficiency CNT-Si heterojunction solar cells by dry gas doping. *Carbon* **2019**, *147*, 164–171. [CrossRef]
7. Kong, X.; Zhang, L.; Liu, B.; Gao, H.; Zhang, Y.; Yan, H.; Song, X. Graphene/Si Schottky solar cells: A review of recent advances and prospects. *RSC Adv.* **2019**, *9*, 863–877. [CrossRef]
8. Gnisci, A.; Faggio, G.; Lancellotti, L.; Messina, G.; Carotenuto, R.; Bobeico, E.; Veneri, P.D.; Capasso, A.; Dikonimos, T.; Lisi, N. The Role of Graphene-Based Derivative as Interfacial Layer in Graphene/n-Si Schottky Barrier Solar Cells. *Phys. Status Solidi* **2018**, *216*, 1800555. [CrossRef]
9. Aderhold, P. Graphite Nanoplatelet Assemblies for Transparent and Catalytic Electrodes in Dye-Sensitized Solar Cells. Ph.D. Thesis, Michigan State University, East Lansing, MI, USA, 2013.
10. Choi, H.; Hwang, S.; Bae, H.; Kim, S.; Kim, H.; Jeon, M. Electrophoretic graphene for transparent counter electrodes in dye-sensitised solar cells. *Electron. Lett.* **2011**, *47*, 281–283. [CrossRef]
11. Yeh, M.H.; Yeh, M.; Yin, L.; Yin, L.; Jheng-Sin, L.; Kuo-Chuan, S.; Kuo-Chuan, H. Nanocomposite graphene/Pt electrocatalyst as economical counter electrode for dye-sensitized solar cells. *Chemelectrochem* **2014**, *1*, 416–425. [CrossRef]
12. Avouris, P.; Xia, F. Graphene applications in electronics and photonics. *MRS Bull.* **2012**, *37*, 1225–1234. [CrossRef]
13. Adhikari, G.C.; Vargas, P.A.; Zhu, H.; Grigoriev, A.; Zhu, P. Tetradic phosphor white light with variable CCT and superla-tive CRI through organ lead halide perovskite nanocrystals. *Nanoscale Adv.* **2019**, *1*, 1791–1798. [CrossRef]
14. Adhikari, G.C.; Thapa, S.; Zhu, H.; Zhu, P. Mg2+Alloyed All-Inorganic Halide Perovskites for White Light-Emitting Diodes by 3D-Printing Method. *Adv. Opt. Mater.* **2019**, *7*, 1900916. [CrossRef]
15. Sohn, Y.; Jun, T.H.; Han, H. Effects of shape and alignment of reinforcing graphite phases on the thermal conductivity and the coefficient of thermal expansion of graphite/copper composites. *Carbon* **2019**, *149*, 152–164. [CrossRef]
16. Liu, B.; Zhang, D.; Lia, X.; He, Z.; Guo, X.; Liu, Z.; Guo, Q. Effect of graphite flakes particle sizes on the microstructure and properties of graphite flakes/copper composites. *J. Alloys Compd.* **2018**, *766*, 382–390. [CrossRef]
17. Liu, B.; Zhang, D.; Li, X.; Guo, X.; Shi, J.; Liu, Z.; Guo, Q. The microstructures and properties of graphite flake/copper com-posites with high volume fractions of graphite flake. *New Carbon Mater.* **2020**, *35*, 58–65. [CrossRef]
18. Han, X.; Huang, Y.; Wang, J.; Zhang, S.; Ding, Z.; Li, T. Fabrication of graphite films/copper composites by vacuum hot pressing for high-efficiency thermal management property. *Compos. Commun.* **2021**, *24*, 100665. [CrossRef]
19. Liu, Q.; Liu, Y.; Tang, S.; Cheng, J.; Chen, Y.; Wang, F.; Lv, Z.; Qu, X. Effects of morphological characteristics of graphite fillers on the thermal conductivity of the graphite/copper composites fabricated by vacuum hot pressing sintering. *Vacuum* **2019**, *167*, 199–206. [CrossRef]
20. Meskinis, S.; Čiegis, A.; Vasiliauskas, A.; Šlapikas, K.; Tamulevicius, S.; Tamuleviciene, A. Optical properties of diamond like carbon films containing copper, grown by high power pulsed magnetron sputtering and direct current magnetron sputtering: Structure and composition effects. *Thin Solid Films* **2015**, *581*, 48–53. [CrossRef]
21. Khamseh, S.; Alibakhshi, E.; Mahdavian, M.; Saeb, M.R.; Vahabie, H.; Kokanyane, N.; Laheurte, P. Magnetron-sputtered copper/diamond-like carbon composite thin films with super anti-corrosion properties. *Surf. Coat. Technol.* **2018**, *333*, 148–157. [CrossRef]
22. Wang, W.; Jia, L.; Lia, H.; Zhoua, H.; Chena, J. Self-organized formation of nano-multilayer structure in the carbon-copper thin film during reactive magnetron sputtering deposition process. *J. Alloys Compd.* **2017**, *722*, 242–249. [CrossRef]
23. Milan, P.B.; Khamseh, S.; Zarintaj, P.; Ramezanzadeh, B.; Badawi, M.; Morisset, S.; Vahabi, H.; Saeb, M.R.; Mozafari, M. Copper-enriched diamond-like carbon coatings promote regeneration at the bone–implant interface. *Heliyon* **2020**, *6*, e03798. [CrossRef] [PubMed]
24. Kavaliauskas, Z.; Marcinauskas, L.; Milieška, M.; Valinčius, V.; Baltušnikas, A.; Žunda, A. Effect of copper content on the properties of graphite-copper composites formed using the plasma spray process. *Surf. Coat. Technol.* **2019**, *364*, 398–405. [CrossRef]
25. Chan, K.-Y.; Tou, T.-Y.; Teo, B.-S. Thickness dependence of the structural and electrical properties of copper films deposited by dc magnetron sputtering technique. *Microelectron. J.* **2006**, *37*, 608–612. [CrossRef]
26. Miranda, F.; Caliari, F.; Essiptchouk, A.; Pertraconi, G. Atmospheric Plasma Spray Processes: From Micro to Nanostructures. In *Atmospheric Pressure Plasma-from Diagnostics to Applications*; BoD—Books: London, UK, 2019. [CrossRef]

27. Xiao, J.-K.; Zhang, W.; Liu, L.-M.; Gan, X.-P.; Zhou, K.-C.; Zhang, C. Microstructure and tribological properties of plasma sprayed Cu-15Ni-8Sn coatings. *Surf. Coat. Technol.* **2018**, *337*, 159–167. [CrossRef]
28. Ranjana, A.; Islam, A.; Pathaka, M.; Kaleem, M.; Anup, K.; Keshri, K. Plasma sprayed copper coatings for improved surface and mechanical properties. *Vacuum* **2019**, *168*, 108834. [CrossRef]
29. Iljinas, A.; Marcinauskas, L.; Stankus, V. In situ deposition of $PbTiO_3$ thin films by direct current reactive magnetron sputtering. *Appl. Surf. Sci.* **2016**, *381*, 6–11. [CrossRef]
30. Christoulis, D.K.; Pantelis, D.I.; De Dave-Fabrègue, N.; Borit, F.; Guipont, V.; Jeandin, M. Effect of substrate temperature and roughness on the solidification of copper plasma sprayed droplets. *Mater. Sci. Eng. A* **2008**, *485*, 119–129. [CrossRef]
31. Meng, Y.; Song, Z.X.; Qian, D.; Dai, W.J.; Wang, J.F.; Ma, F.; Li, Y.H.; Xu, K.W. Thermal stability of RuZr alloy thin films as the diffusion barrier in Cu metallization. *J. Alloy. Compd.* **2013**, *588*, 461–464. [CrossRef]
32. Patwary, M.A.; Saito, K.; Guo, Q.; Tanaka, T. Influence of oxygen flow rate and substrate positions on properties of Cu-oxide thin films fabricated by radio frequency magnetron sputtering using pure Cu target. *Thin Solid Films.* **2019**, *675*, 59–65. [CrossRef]
33. Ageev, A.G.; Kavyrshin, D.I.; Sargsyan, M.; Gadzhiev, M.K.; Chinnov, V.F. Determination of graphite sublimation rate in high enthalpy plasma flow using 'laser knife' method. *Int. J. Heat Mass Transf.* **2017**, *107*, 146–153. [CrossRef]
34. Kale, A.S.; Nemeth, W.; Perkins, C.L.; Young, D.; Marshall, A.; Florent, K.; Kurinec, S.K.; Stradins, P.; Agarwal, S. Thermal Stability of Copper-Nickel and Copper-Nickel Silicide Contacts for Crystalline Silicon. *ACS Appl. Energy Mater.* **2018**, *1*, 2841–2848. [CrossRef]
35. Wang, C.-Y.; Yuan, F.-W.; Hung, Y.-C.; Su, Y.-W.; Tuan, H.-Y. In-situ TEM and XRD analysis of microstructures changes in solution-grown copper silicide nanowires array for field emitters. *J. Alloy. Compd.* **2018**, *735*, 2373–2377. [CrossRef]
36. Muhlbacher, M.; Greczynski, G.; Sartory, B.; Schalk, N.; Lu, J.; Petrov, I.; Greene, J.E.; Hultman, L.; Mitterer, C. Enhanced $Ti_{0.84}Ta_{0.16}N$ diffusion barriers, grown by a hybrid sputtering technique with no substrate heating, between Si(001) wafers and Cu overlayers. *Sci. Rep.* **2018**, *8*, 1–9. [CrossRef] [PubMed]